

2018-07-01

# Downhill exercise alters immunoproteasome content in mouse skeletal muscle

---

Cory W Baumann, Dongmin Kwak, Deborah A Ferrington, LaDora V Thompson. 2018.

"Downhill exercise alters immunoproteasome content in mouse skeletal muscle." *Cell Stress & Chaperones*, Volume 23, Issue 4, pp. 507 - 517. <https://doi.org/10.1007/s12192-017-0857-y>

<https://hdl.handle.net/2144/40890>

*"Downloaded from OpenBU. Boston University's institutional repository."*

TITLE

Downhill Exercise Alters Immunoproteasome Content in Mouse Skeletal Muscle

AUTHORS

Cory W. Baumann<sup>1</sup>, Dongmin Kwak<sup>2</sup>, Deborah A. Ferrington<sup>3</sup>, LaDora V. Thompson<sup>2</sup>

LABORATORY AND INSTITUTE

<sup>1</sup>Department of Rehabilitation Medicine,  
University of Minnesota, Minneapolis, Minnesota, USA

<sup>2</sup>Department of Physical Therapy and Athletic Training  
Boston University, Boston, Massachusetts, USA

<sup>3</sup>Department of Ophthalmology and Visual Neuroscience,  
University of Minnesota, Minneapolis, Minnesota, USA

CORRESPONDENCE

Cory W. Baumann  
Department of Rehabilitation Medicine  
University of Minnesota  
Minneapolis, Minnesota, USA  
Email: cbaumann@umn.edu  
Phone: 612-626-5022

## ABSTRACT

Content of the immunoproteasome, the inducible form of the standard proteasome, increases in atrophic muscle suggesting it may be associated with skeletal muscle remodeling. However, it remains unknown if the immunoproteasome responds to stressful situations that do not promote large perturbations in skeletal muscle proteolysis. The purpose of this study was to determine how an acute bout of muscular stress influences immunoproteasome content. To accomplish this, wildtype (WT) and immunoproteasome knockout *lmp7<sup>-/-</sup>/mecl1<sup>-/-</sup>* (L7M1) mice were run downhill on a motorized treadmill. Soleus muscles were excised 1 and 3 days post-exercise and compared to unexercised muscle (control). *Ex vivo* physiology, histology and biochemical analyses were used to assess the effects of immunoproteasome knockout and unaccustomed exercise. Besides L7M1 muscle being LMP7/MECL1 deficient, no other major biochemical, histological or functional differences were observed between the control muscles. In both strains, the downhill run shifted the force-frequency curve to the right and reduced twitch force, however did not alter tetanic force or inflammatory markers. In the days post-exercise, several of the proteasome's catalytic subunits were upregulated. Specifically, WT muscle increased LMP7 while L7M1 muscle instead increased  $\beta 5$ . These findings indicate that running mice downhill results in subtle contractile characteristics that correspond to skeletal muscle injury, yet does not appear to induce a significant inflammatory response. Interestingly, this minor stress activated the production of specific immunoproteasome subunits; that if knocked out, were replaced by components of the standard proteasome. These data suggest that the immunoproteasome may be involved in maintaining cellular homeostasis.

Key Words: degradation, eccentric contractions, oxidative stress, muscle function

## INTRODUCTION

Unaccustomed exercise is known to injure skeletal muscle. Eccentric contractions, which decelerate limbs during exercise, cause muscle injury due to their intrinsic capacity to produce high levels of stress. In the laboratory, contraction-induced injury is commonly studied by having mice perform strenuous downhill exercise or isolated high-force eccentric contractions. The severity of the injury is largely determined by the amount of muscle lengthening and the force it generates during the eccentric exercise or contraction protocol (Brooks et al. 1995; Warren et al. 1993a). Functionally, eccentric contraction-induced injury in mouse skeletal muscle results in immediate strength loss that can take several days or even weeks to fully recover (Baumann et al. 2016c; Ingalls et al. 1998a; Rathbone et al. 2003). It is generally accepted that short-term strength deficits result from a failure in voltage-gated sarcoplasmic reticulum (SR) calcium release that partially stems from disruptions in key excitation-contraction (EC) coupling proteins (Baumann et al. 2014b; Corona et al. 2010; Ingalls et al. 1998b). Then after, strength deficits are mainly explained by reductions in the muscle's contractile proteins, myosin and actin (Ingalls et al. 1998a). Complete recovery of strength is therefore a combined effort of replacing or refolding EC coupling and contractile proteins through increased protein synthesis rates (Baumann et al. 2016d; Lowe et al. 1995), satellite cell activity (Rathbone et al. 2003) and heat shock proteins (Baumann et al. 2016c; McArdle et al. 2004), but also the removal of any damaged (or modified) proteins that may be present following the unaccustomed exercise (Lowe et al. 1995).

The ubiquitin-proteasome system is one of the primary intracellular protein degradation pathways in skeletal muscle and involves polyubiquitination of target proteins and their subsequent proteolysis by the standard proteasome (Lecker et al. 2006; Lecker et al. 1999). The standard proteasome (26S) is composed of a cylindrical catalytic (20S) core that can be capped at one or both ends with ATP-dependent PA700 regulatory complexes (19S) (Bedford et al. 2010; Coux et al. 1996; Klotzel 2001; Tanaka 2009). The regulatory complexes serve as gates, recognizing and transferring protein's into the 20S core. The 20S core consists of four rings that contain seven subunits each, two outer rings composed of alpha subunits ( $\alpha$ 1- $\alpha$ 7) and two inner rings of beta subunits ( $\beta$ 1- $\beta$ 7). Among the  $\beta$  subunits,  $\beta$ 1,  $\beta$ 5 and  $\beta$ 2 are catalytically active and cleave after acidic, hydrophobic and basic amino acid residues, respectively (Bedford et al. 2010; Coux et al. 1996; Klotzel 2001; Tanaka 2009). Several components of the ubiquitin-proteasome system have been shown to increase during atrophic states (e.g., denervation) and following unaccustomed exercise (Attaix et al. 2005; Baumann et al. 2016b; Reid 2005; Willoughby et al. 2003), demonstrating that the standard proteasome is an essential mediator of skeletal muscle remodeling (Reid 2005).

In the presence of interferon gamma ( $\text{IFN}\gamma$ ) or tumor necrosis factor alpha ( $\text{TNF}\alpha$ ) the immunoproteasome, a variant of the standard proteasome, is expressed (Bhattarai et al. 2016; Klotzel 2001; Tanaka and Kasahara 1998). Structurally, the immunoproteasome is very similar to the standard proteasome, except  $\beta$ 1,  $\beta$ 5 and  $\beta$ 2 are replaced with the inducible subunits LMP2 ( $\beta$ 1i), LMP7 ( $\beta$ 5i) and MECL1 ( $\beta$ 2i), and its catalytic core can associate with PA28 (11S), an ATP-independent regulatory complex (Ferrington and Gregerson 2012; Klotzel 2001; Tanaka

2009). The immunoproteasome has several well-characterized, immune-related functions that include regulating antigen presentation and cytokine expression (Bhattarai et al. 2016; Kloetzel 2001; Tanoka and Kasahara 1998), but it also possesses the ability to degrade oxidized and misfolded proteins (Cui et al. 2014; Ferrington and Gregerson 2012; Seifert et al. 2010). Therefore, diseases mechanistically linked to inflammation and/or oxidation are often associated with altered immunoproteasome expression and function, making the immunoproteasome a potential therapeutic target (Ferrington and Gregerson 2012). In fact, disease progression in mouse models of colitis (Basler et al. 2010), systemic lupus erythematosus (Ichikawa et al. 2012), diabetes, and rheumatoid arthritis (Muchamuel et al. 2009) can all be attenuated by selectively inhibiting the immunoproteasome's catalytic subunit LMP7.

In skeletal muscle, immunoproteasome content increases across various catabolic conditions, as seen with aging (Ferrington et al. 2005; Husom et al. 2004), denervation (Liu et al. 2016), muscular dystrophy (Chen et al. 2014; Farini et al. 2016), and idiopathic inflammatory myopathies (Bhattarai et al. 2016). These data support that similar to the standard proteasome, the immunoproteasome is involved in regulating and possibly maintaining cellular homeostasis in skeletal muscle. However, it is currently unknown if the immunoproteasome responds to stressful situations that do not promote large perturbations in skeletal muscle proteolysis (i.e., significant atrophy). The goals of this study were twofold, (1) determine if an acute bout of muscular stress stimulates upregulation of immunoproteasome content and (2) assess how the muscle reacts when it is deficient in two of the three inducible subunits. To accomplish this, we subjected wildtype (WT) and *Imp7<sup>-/-</sup>/mecl1<sup>-/-</sup>* double knockouts (L7M1) mice to a single session of unaccustomed exercise and analyzed proteasome content (i.e., standard proteasome and immunoproteasome) within the soleus muscle over the impending days. Using this design we were able to document how the immunoproteasome responded to exercise-induced injury and if the proteasome was differentially affected in skeletal muscle of L7M1 mice.

## METHODS

### **Animals**

Male 8-16 week-old WT and L7M1 mice with a C57BL/6 genetic background were used in this study (Hussong et al. 2011; Liu et al. 2016; Schuld et al. 2015). Mice were housed in groups of no more than 4 animals per cage, supplied with food and water *ad libitum* and maintained in a room at 20-23°C with a 12-h photoperiod. During the final procedure (i.e., *Ex vivo* muscle preparation and contractility measurements), mice were anesthetized by an intraperitoneal injection of ketamine/xylazine (100 mg/kg ketamine, 10 mg/kg xylazine), with supplemental doses given as required. Following the completion of this procedure, mice were euthanized by exsanguination while under anesthesia. All animal procedures were approved by the Institutional Animal Care and Use Committee at the University of Minnesota.

### **Experimental design**

In attempt to induce skeletal muscle injury, WT and L7M1 mice were exercised by running on a motorized treadmill at a negative grade (i.e., downhill). Mice were euthanized one (day 1) or three (day 3) days following the exercise bout and compared to mice that did not exercise (control). These time points were selected based on previous reports that demonstrated markers of contraction-induced skeletal muscle injury are evident in the muscles of the posterior compartment (soleus, plantaris and gastrocnemius) after mice run downhill (López et al. 2016; Lueders et al. 2011; Lynch et al. 1997). From these muscles, the soleus was specifically selected for testing because its accessibility, structure and size make it ideal for studying contractile physiology in an *ex vivo* model (Baumann et al. 2016b; Warren et al. 1993b). However, because the soleus is relatively small (i.e., 8-12 mg), it is difficult to follow up with numerous biochemical or histological experiments. Therefore, to optimize the amount of sample that could be used, the left soleus of each mouse was used for physiology and biochemistry while the right was prepped for histology.

## **Experimental methodology**

### *Body composition*

Because we have previously observed L7M1 mice weigh significantly more than age-matched WT mice (Liu et al. 2016), body fat percentage was measured on a subset of WT and L7M1 mice before any testing took place. Briefly, at 8-10 weeks of age, mice were anesthetized with isoflurane, carefully placed on a specimen tray and scanned using a Lunar PIXImus densitometer (GE Lunar Corporation, Madison, WI, USA) according the specifications set by the manufacturer.

### *Treadmill protocol (downhill run)*

Mice designated to exercise were first allowed 5 min to ambulate freely on a motorized treadmill (Exer-6M, Columbus Instruments, Columbus, OH) set at  $-10^{\circ}$  grade with no belt speed in order to become familiarized with the laboratory environment. Following this stationary stage, mice warmed-up by running for 6 min at a  $-22^{\circ}$  grade, in which belt speed increased from 5 to 13 m/min. Mice were then given a 3 min rest period before performing a 70 min downhill running protocol that consisted of 10 stages at a  $-22^{\circ}$  grade. Each stage began with a 1 min acceleration period (from 5 to 13 m/min), followed by 6 min of constant running at 13 m/min. To prevent exhaustion and ensure the mice could finish the protocol, each stage was separated with a 3 min rest period. Mice were occasionally prodded with a 6 inch cotton tipped applicator to encourage continuous running; electric shock was not used because mice generally responded to a gentle tap on the tail or hindquarters.

### *Ex vivo muscle preparation and contractility measurements*

The soleus muscle from the left hindlimb of the anesthetized mouse was dissected free and studied using an *ex vivo* preparation, similar to that described previously (Baumann et al. 2016b). Following excision, the muscle was mounted in an organ bath containing a Krebs-Ringer buffer (pH 7.3), which was equilibrated with 95% O<sub>2</sub>-5% CO<sub>2</sub> gas and maintained at 25°C via a circulating water system. The distal tendon was attached by a silk suture and secured to a fixed support, and the proximal tendon was attached to the lever arm of a servomotor system (300B; Aurora Scientific Inc., Aurora, ON, Canada). Optimal muscle length ( $L_0$ ) was set with a series of twitch stimulations (0.2 ms pulse at 30 V). Three minutes after  $L_0$  was determined, the muscle performed a final twitch contraction followed by a force-frequency protocol that included seven isometric contractions (600 ms train of 0.2 ms pulses at 10, 30, 60, 80, 100, 120 and 150 Hz), all separated by a 3 min rest period. For analysis, the final twitch was recorded as peak isometric twitch force ( $P_t$ ), whereas the highest recorded force during the force-frequency protocol was defined as peak isometric tetanic force ( $P_o$ ).

The soleus muscle was then removed from the bath assembly, trimmed, weighed, frozen in liquid nitrogen and stored at -80°C. Muscle mass and  $L_0$  were used to calculate physiological cross-sectional area (CSA), with 0.71 and 1.06 representing the fiber length-to-muscle length ratio and average density, respectively (Brooks and Faulkner 1988; Méndez and Keys 1960). To obtain relative (i.e., specific) force, absolute force in Newtons (N) was divided by physiological CSA and expressed in N·cm<sup>-2</sup>.

#### *Histology and immunohistochemistry*

After the left soleus muscle was prepped for *ex vivo* physiology, the right soleus muscle was excised, embedded in a tissue freezing medium, immediately frozen in 2-methylbutane cooled in liquid nitrogen and stored -80°C.

Transverse, serial sections at 10 µm were cut through the mid-belly of the soleus muscle using a cryostat (Leica CM3050S, Nussloch, Germany) and saved for staining. Slides were later processed using a hematoxylin and eosin (H&E) stain (ScyTek Laboratories, Logan, UT, USA) or prepared for immunohistochemistry.

Slides using H&E were stained according to the manufacturer's recommendations, dehydrated, mounted and visualized at 10X with a Nikon Eclipse E400 microscope (Nikon, Tokyo, Japan). The CSA of approximately 200 fibers per muscle were measured using ImageJ analysis software (National Institutes of Health, Bethesda, MD, USA).

Immunohistochemistry was conducted as previously described (Wang et al. 2016). Briefly, slides were washed with phosphate-buffered saline (PBS) for 5 min and fixed with a 10% formaldehyde solution for 10 min. After fixation, slides were washed, blocked with 5% bovine serum albumin (BSA) dissolved in PBS for 30 min and rewashed with PBS. The slides were then incubated with a primary antibody (CD45, 1:30, R&D Systems, Minneapolis, MN, USA) diluted in 5% BSA dissolved in PBS for 1 h and washed as previously stated. Slides were incubated with a secondary antibody (Alexa Fluor 555-conjugated antibody, 1:500, Life Technologies, Gaithersburg, MD, USA)

diluted in 5% BSA dissolved in PBS for 30 min and rewashed. After the wash, slides were incubated with 4', 6'-diamidino-2-phenylindole (DAPI, 1:40000, Life Technologies) in 5% BSA dissolved in PBS for 10 min. Following incubation, slides were washed, dehydrated, mounted and visualized at 10X using a ZEISS microscope (Carl Zeiss, Oberkochen, Germany). Positively stained CD45 cells from three random fields per slide were quantified and expressed relative to the number of stained nuclei.

#### *Soleus muscle homogenization*

The left soleus muscle from each mouse was homogenized in an ice-cold RIPA lysis buffer (Thermo Scientific, Rockford, IL, USA) that was supplemented with a protease inhibitor cocktail (Thermo Scientific) and 1%  $\beta$ -mercaptoethanol. Muscle homogenates were centrifuged at 8,160 g for 10 min at 4°C. Protein content was quantified in triplicate using a reducing agent compatible bicinchoninic acid (BCA) assay (Thermo Scientific) with BSA as a standard. Homogenates were then aliquoted and saved at -20°C for immunoblotting and enzyme-linked immunosorbent assays (ELISAs).

#### *Immunoblots (Western blots) and immunoassays (ELISAs)*

A portion of the muscle homogenate was then diluted in a loading buffer and heated for 5 min. For each sample, an equal amount of protein was loaded onto an 11% sodium dodecyl sulfate (SDS) polyacrylamide gel and separated according to molecular weight (100 V for 40 min, 150 V for 60 min). For each primary antibody (**Supplementary Table 1**) the optimal protein concentration was predetermined and ranged from 5-15  $\mu$ g. Proteins were transferred to a PDVF membrane using a wet transfer system at 100 V for 70 min (Bio-Rad Laboratories, Hercules, CA, USA). Membranes were allowed to dry overnight and then were reactivated in methanol and blocked in 5% nonfat dried milk dissolved in tris-buffered saline containing 0.1% Tween-20 (TBS-T) for at least 1 h at room temperature the following day. After the block, membranes were probed with primary antibodies corresponding to subunits of the standard proteasome and/or immunoproteasome (**Supplementary Table 1**). The primary antibodies were diluted in 0.2% nonfat dried milk dissolved in TBS-T for 2 h at room temperature or overnight at 4°C on an orbital shaker. Following incubation in the primary antibodies, membranes were washed with TBS-T and then probed with the appropriate secondary antibody (goat anti-rabbit IgG, 1:10000, Santa Cruz or goat anti-mouse IgG, 1:10000, Thermo Scientific) diluted in 5% nonfat dried milk dissolved in TBS-T for 1 h at room temperature with shaking and washed as previously stated. Membranes were then treated with an enhanced chemiluminescent solution (Thermo Scientific) prior to detection using a BioRad ChemiDoc XRS imaging station (Bio-Rad Laboratories) and analyzed by volume using QuantityOne software (Bio-Rad Laboratories). For data analysis, content from each protein of interest was normalized to glyceraldehyde 3-phosphate dehydrogenase (GAPDH) content.

Immunoblotting was also performed to quantify carbonylated protein content using an OxyBlot protein oxidation detection kit (Millipore, Temecula, CA, USA). Briefly, a portion of the muscle homogenate was denatured and

derivatized using SDS and 2,4-dinitrophenylhydrazine (DNP-hydrazine), respectively, at room temperature for 15 min. A neutralizing solution was then added, and for each sample an equal amount of protein (5 µg) was loaded, separated and transferred to a PVDF membrane as mentioned above. Membranes were blocked in 1% BSA dissolved in PBS containing 0.05% Tween-20 (PBS-T) for at least 1 hour at room temperature. After the block, the membranes were probed with an anti-DNP primary antibody diluted in 1% BSA dissolved in PBS-T for 1 h at room temperature on an orbital shaker. Following incubation in the primary antibody, membranes were washed with PBS-T and then probed with the corresponding secondary antibody diluted in 1% BSA dissolved in PBS-T for 1 hour at room temperature with shaking and washed as previously stated. Membranes were then treated, imaged and analyzed as mentioned above.

A portion of the muscle homogenate was also diluted with DDI H<sub>2</sub>O in preparation for ELISAs. Mouse ELISA kits for monocyte chemoattractant protein 1 (MCP1) and TNF $\alpha$  were then completed according to the manufacture's specifications (Thermo Scientific). Briefly, an equal amount of protein (50 µg) was loaded for every sample and assessed in duplicate. Total content was determined based on the standard curve for either MCP1 or TNF $\alpha$ . For analysis, the duplicates were averaged and expressed in pg/ml.

### **Statistical analyses**

An independent t-test was first used to determine if there were differences between control WT and L7M1 mice. A two-way factorial ANOVA (strain x time) was then utilized to assess how WT and L7M1 mice responded to the downhill run. For protein content of LMP7 and MECL1, a one-way ANOVA had to be used because these proteins are not expressed in L7M1 mice. Values were set relative to their respective control group for all analyses when a time factor was included (i.e., control vs. 1 day vs. 3 day), and graphed as a fraction or % of the control group, unless stated otherwise. In the event of a significant ANOVA, a Fisher's least significant difference (LSD) post hoc test was performed. An  $\alpha$ -level of <0.05 was used for all analyses. Values are presented in mean $\pm$ SEM. All statistical testing was performed using SigmaPlot version 11.0 (Systat Software, San Jose, CA, USA).

## **RESULTS**

### **Body composition, soleus wet weight and fiber CSA**

On average, control L7M1 mice weighed ~14%% more than their WT counterparts (p=0.011) (**Fig. 1A**) and possessed ~6% more body fat (p<0.001) (**Fig. 1B**). Despite these characteristics, soleus wet weight did not differ between WT and L7M1 control mice (p=0.13) (**Fig. 1C**), which was confirmed by assessing soleus fiber CSA (p=0.22) (**Fig. 1D**). These data suggest LMP7/MECL1 double knockout results in a heavier and fatter mouse phenotype.

### **Soleus function and contractility**

When normalized to physiological CSA,  $P_t$  and  $P_o$  did not differ between WT and L7M1 control muscle ( $p \geq 0.79$ ) (**Fig. 1E, 1F**). To determine the extent of injury caused by the downhill run,  $P_t$  and  $P_o$  were also assessed 1 and 3 days post-exercise (**Fig. 2A, 2B**). Running downhill at a  $-22^\circ$  grade for 70 min at 13 m/min did not impair soleus  $P_o$  in the exercised WT or L7M1 groups ( $p=0.33$ ). In contrast to that of  $P_o$ ,  $P_t$  was significantly depressed after the downhill run (17%,  $p=0.022$ ). Specifically, 1 day post-exercise  $P_t$  was reduced 10 and 25% in WT and L7M1 muscle, respectively. Although  $P_t$  appeared to be depressed to a greater extent in L7M1 muscle, no significant interaction was present ( $p=0.28$ ). By day 3,  $P_t$  remained  $\sim 10\%$  down in WT muscle and had recovered to an 8% deficit in L7M1 muscle, which together did not differ when compared to that of the control or day 1 muscles ( $p \geq 0.22$ ).

Because reductions in  $P_t$  most likely correspond to changes in calcium handling, the  $P_t$  to  $P_o$  ratio and  $\text{Freq}_{50}$  were also analyzed (**Fig. 2C-2E**). These are important contractile parameters that are altered following eccentric contractions (Chan et al. 2007; Chan et al. 2008; Ingalls et al. 2004). The  $P_t$  to  $P_o$  ratio is calculated by dividing  $P_t$  by  $P_o$ , and has been used as an indirect marker of EC uncoupling. Traditionally, a more pronounced reduction in  $P_t$  relative to  $P_o$  indicates greater EC coupling failure (Baumann et al. 2016c; Ingalls et al. 2004; Jones et al. 1982). The  $\text{Freq}_{50}$  (also referred to  $\text{EC}_{50}$ ) is the stimulation frequency at which 50% maximal force is generated and was determined by fitting a Hill sigmoidal curve to the force-frequency data for each muscle. As with the  $P_t$  to  $P_o$  ratio, changes in the  $\text{Freq}_{50}$  may represent alterations in calcium handling. A rightward shift in the force-frequency curve (i.e., an increase in the  $\text{Freq}_{50}$ ) could indicate reduced sensitivity of the contractile proteins to calcium and/or EC coupling failure (Chan et al. 2008). The  $P_t$  to  $P_o$  ratio and  $\text{Freq}_{50}$  mimicked that of  $P_t$ , in which both were significantly different from control muscle 1 day post-exercise ( $p \leq 0.015$ ), but were similar between strains ( $p \geq 0.19$ ) (**Fig. 2C-2E**). Specifically, the  $P_t$  to  $P_o$  ratio decreased and  $\text{Freq}_{50}$  increased 1 day post-exercise (i.e., shifted to the right), and began to recover by day 3. Together, the changes observed in  $P_t$ , the  $P_t$  to  $P_o$  ratio and  $\text{Freq}_{50}$  all indicate that the soleus muscle was modestly injured following the downhill run. Peak force values expressed in  $\text{N} \cdot \text{cm}^{-2}$  and the  $P_t$  to  $P_o$  ratios are listed in **Supplementary Table 2**.

### **Proteasome content**

To analyze how the stress of downhill running affected proteasome expression and if LMP7/MECL1 deficiency altered this response, content of several standard proteasome and immunoproteasome subunits were assessed (**Fig. 3A-3H**).

The first proteins to be analyzed were the  $\beta$  subunits, the proteins responsible for the proteasome's catalytic activities. They include the standard subunits (i.e.,  $\beta_1$ ,  $\beta_5$ ) and the inducible subunits (i.e., LMP7/ $\beta_5i$ , MECL1/ $\beta_2i$ ), which correspond to the standard proteasome and immunoproteasome, respectively. No strain differences were

observed in  $\beta 1$  or  $\beta 5$  content in control muscle ( $p \geq 0.45$ ) (**Fig. 3H**). And as expected, L7M1 muscle did not express LMP7 or MECL1 (**Fig. 3H**). After the downhill run, both LMP7 and MECL1 content increased in WT muscle (**Fig. 3A, 3B**). When compared to WT control muscle, LMP7 was 24% greater at day 1 ( $p = 0.033$ ) while MECL1 tended to be higher following the exercise ( $p = 0.091$ ). Content of  $\beta 1$  and  $\beta 5$  also responded to the downhill run (**Fig. 3C, 3D**), in particular that of  $\beta 5$  from L7M1 muscle. Specifically,  $\beta 5$  content increased 34 and 62% over that of L7M1 control muscle 1 and 3 days post-exercise ( $p = 0.002$ ), and was significantly greater than that observed in the exercised WT muscle ( $p = 0.009$ ). As with MECL1,  $\beta 1$  tended to increase following the downhill run ( $p = 0.086$ ), however this effect was similar between strains ( $p = 0.65$ ).

Because several of the proteasome's catalytic subunits increased after the downhill run, we also examined content of PA28 $\alpha$  and Rpt1, subunits of the proteasome's regulatory complexes (**Fig. 3E, 3F**). In which, PA28 $\alpha$  is a subunit of the immunoproteasome's regulatory complex PA28 while Rpt1 is a subunit of the standard proteasome's regulatory complex PA700. As with the catalytic subunits, no differences were detected between strains in PA28 $\alpha$  or Rpt1 content in control muscle ( $p \geq 0.18$ ) (**Fig. 3H**). In contrast to that of LMP7 and MECL1, PA28 $\alpha$  was not affected by the exercise in WT muscle, nor was it altered in L7M1 muscle ( $p \geq 0.25$ ) (**Fig. 3E**). Interestingly, Rpt1 content did respond to the downhill run, but in opposing directions between strains (**Fig. 3F**). In WT muscle Rpt1 content appeared to increase, while in L7M1 muscle it decreased. Although no interaction was detected ( $p = 0.19$ ), Rpt1 content was significantly different between strains in the days post-exercise ( $p = 0.029$ ).

To further investigate the changes observed in the proteasome, we next determined  $\alpha 7$  content (**Fig. 3G**). The  $\alpha$  subunits ( $\alpha 1$ - $\alpha 7$ ) are constitutively expressed in both the standard proteasome and immunoproteasome, and therefore are considered a reliable measure of the total proteasome (Hussong et al. 2010). However,  $\alpha 7$  did not differ between strains in control muscle or change as a result of the downhill run ( $p \geq 0.34$ ).

Together, no measureable differences in  $\beta 1$ ,  $\beta 5$ , PA28 $\alpha$ , Rpt1 or  $\alpha 7$  protein content were present between WT and LMP7/MECL1 deficient muscle in the unstressed state, similar to what we have recently reported in 5-7 month old mice (Liu et al. 2016). However, when stressed by a bout of downhill exercise, WT muscle significantly upregulated LMP7 content while L7M1 muscle instead increased  $\beta 5$  content.

## Inflammation

Because immunoproteasome expression and eccentric-contraction induced injury are associated with inflammation (Bhattarai et al. 2016; Lowe et al. 1995; Pizza et al. 2002), content of MCP1 and TNF $\alpha$  were measured in both the control and exercised soleus muscles (**Fig. 4A, 4B**). These proinflammatory markers were specifically selected based on previous downhill run studies demonstrating an upregulation in mice muscle (López et al. 2016). In the present study, MCP1 and TNF $\alpha$  content did not differ between control muscle ( $p \geq 0.52$ ), nor did content significantly increase as a result of the downhill run ( $p \geq 0.31$ ) (**Fig. 4A, 4B**). In addition to measuring proinflammatory cytokine

production, histological sections were stained for CD45, a marker of leukocyte infiltration. Quantification of CD45 positive cells was similar to that of MCP1 and TNF $\alpha$  content; that is, no differences were detected between controls or following the downhill run ( $p \geq 0.12$ ) (**Fig. 4C, Supplementary Fig. 1A**). These data suggest that the stress associated with the downhill run did not induce a significant inflammatory response within the soleus muscle of WT or L7M1 mice, at least from the time points measured in the present study. MCP1 and TNF $\alpha$  content in pg/ml and the percentage of positively stained CD45 cells are listed in **Supplementary Table 2**.

### **Protein carbonylation**

To assess if the alterations observed in proteasome content were a result of oxidative damage caused by the downhill run, we measured protein carbonylation in total (i.e., whole lane) and for three prominent bands (**Fig. 5A-5E**). These bands were located at approximately 220, 40 and 30 kDa. No differences were observed between strains or as a result of the exercise in total, or at the bands near 220 or 40 kDa ( $p \geq 0.25$ ) (**Fig. 5A-5C**). In contrast, protein carbonylation at the 30 kDa band significantly increased 36 and 45% in the WT and L7M1 muscle 1 day post-exercise ( $p=0.014$ ), respectively, however no differences were observed between the strains ( $p=0.78$ ) (**Fig. 5D**). By day 3, protein carbonylation of this band was similar to that of control muscle ( $p=0.24$ ). Despite the increase observed at 30 kDa, the downhill run did not drastically alter carbonylation content among total proteins or within prominent bands of larger molecular weight proteins.

## DISCUSSION

The functional roles of the immunoproteasome other than generating peptides for antigen presentation have just recently begun to emerge. In skeletal muscle, immunoproteasome content increases across various catabolic conditions, indicating it may be involved in cellular homeostasis. However, it remains unclear if the immunoproteasome responds to stressful situations that do not promote large perturbations in skeletal muscle proteolysis. In the present study we assessed how a single bout of unaccustomed exercise, in which no large-scale atrophy occurs, affects immunoproteasome content in mouse skeletal muscle. Here, we show LMP7 content increases post-exercise; in addition, demonstrate that  $\beta 5$  is up-regulated when LMP7/MECL1 is knocked out. Two key conclusions can be deduced from these data. First, immunoproteasome content within skeletal muscle is sensitive to unaccustomed exercise supporting its role in maintaining cellular homeostasis. Second, the immunoproteasome and standard proteasome are dynamic protein complexes whereby structural alterations in one may influence the composition of the other.

Eccentric exercise or isolated eccentric contractions injure skeletal muscle as evidenced by decrements in the muscle's force producing capacity (Baumann et al. 2014b; Lowe et al. 1995; Warren et al. 1993b). To injure the soleus muscle, we subjected mice to a downhill running protocol, a common laboratory method used to bias human (Baumann et al. 2014a; Schwane et al. 1982) and rodent (Armstrong et al. 1983; Lueders et al. 2011; Lynch et al.

1997) skeletal muscle to perform eccentric contractions. Several functional features indicative of eccentric contraction-induced injury were observed following our downhill running protocol. These included reductions in  $P_t$  and the  $P_t$  to  $P_o$  ratio, and an increase in  $Freq_{50}$  that was also observed by a rightward shift in the force-frequency curves. It is thought that these functional features, often referred to as low-frequency fatigue, are due to alterations in calcium handling or more specifically, EC coupling failure (Chan et al. 2008; Ingalls et al. 2004; Jones et al. 1982; Westerblad et al. 1993). However, it must be noted that these changes were marginal when compared to protocols that utilize maximal isolated eccentric contractions (Baumann et al. 2016c; Lowe et al. 1995), which is supported by the fact  $P_o$  was not impaired by the downhill run. Together, the contractile features observed following the downhill run indicate that the soleus muscle was modestly injured in our cohort of WT and L7M1 mice.

Despite the downhill run only causing subtle deficits to muscular function, it was sufficient to alter proteasome content in the days post-exercise. Alterations in the proteasome were largely observed among the catalytic subunits and appeared to be dependent on strain. WT muscle transiently upregulated LMP7 while L7M1 muscle instead increased  $\beta 5$  content. Although this is the first report to demonstrate LMP7 content increases in skeletal muscle due to unaccustomed exercise, previous studies have observed LMP7 is upregulated in numerous atrophic models. In fact, data from several laboratories, including our own, have shown elevated LMP7 content in aged (Ferrington et al. 2005; Husom et al. 2004), denervated (Liu et al. 2016), dystrophic (Chen et al. 2014; Farini et al. 2016) and myopathic (Bhattarai et al. 2016) skeletal muscle. Most of these reports also demonstrated LMP2 and/or MECL1 content, the immunoproteasome's other catalytic subunits, increased in parallel to LMP7. In the present study, MECL1 content tended to be higher following the downhill run, peaking 1 day post-exercise, similar to LMP7 content. Collectively, these data indicate the immunoproteasome, particularly its catalytic subunits (i.e., inducible subunits: LMP7, MECL1 and LMP2) within skeletal muscle increase in response to age, disuse, disease and unaccustomed eccentric exercise.

The principle role of the inducible subunits is to generate peptides with high MHC I binding affinity for antigen presentation (Kloetzel 2001; Tanaka and Kasahara 1998). Thus, in any model that triggers an inflammatory response within the muscle, immune cells will be present and contribute to immunoproteasome content. In order to determine if the increase we observed in LMP7 was simply due to infiltrating immune cells, content of MCP1 and  $TNF\alpha$ , and the percentage of CD45 positivity stained cells were assessed. As anticipated from the relatively minor changes observed in muscular function, none of these inflammatory markers were altered 1 or 3 days after the downhill run. These findings suggest that LMP7 was upregulated by the myofibers rather than infiltrating immune cells. In favor of this concept, several groups have reported LMP7 and/or LMP2 are present or can be induced in non-immune cells including human myoblast and myofibers (Bhattarai et al. 2016), and C2C12 cells (i.e., mouse myoblasts) (Cui et al. 2014). Together, these data support the assumption that the myofibers were expressing LMP7 after the downhill run, despite inflammatory markers remaining reasonably stable.

Degrading oxidized proteins is thought to be another important role of the inducible subunits (Cui et al. 2014; Ferrington and Gregerson 2012; Seifert et al. 2010). Therefore, in the present study, LMP7 may have been upregulated to counteract an increase in protein carbonylation. The introduction of carbonyl groups into proteins is a non-enzymatic modification that occurs either by direct interaction with reactive oxygen species (ROS) or indirectly through the peroxidation of lipids, and is thought to be a good estimate of oxidative damage (Dalle-Donne et al. 2003). In the days following the injury, the total amount of carbonylated proteins did not increase in either strain. However, we have previously suggested that specific modifications may be missed if oxidative stress is measured too globally (Baumann et al. 2016a). Therefore, we assessed three prominent bands (220, 40 and 30 kDa) and found that protein carbonyls did indeed increase, but only for proteins with low molecular weights (i.e., 30 kDa). Interestingly, the changes observed in protein carbonylation paralleled that of LMP7 content, which may indicate LMP7 was upregulated to degrade these oxidized proteins. Several previous reports support this concept. For instance, differentiating C2C12 cells have more oxidized proteins following chemical inhibition of LMP7 and LMP2 (Cui et al. 2014), while several studies have observed content of LMP7 and/or LMP2 are elevated in aged (Ferrington et al. 2005; Husom et al. 2004) and dystrophic (Chen et al. 2014; Farini et al. 2016) skeletal muscle. Taken as a whole, these findings demonstrate that the inducible subunits within skeletal muscle respond to both acute and chronic oxidative stress.

The standard catalytic subunits also function to degrade oxidized proteins (Davies 2001; Jung and Grune 2008). Indeed,  $\beta 5$  was drastically upregulated 1 and 3 days post-exercise in L7M1 muscle. This finding is particularly interesting as both LMP7 and  $\beta 5$  perform chymotrypsin-like activity cleaving after hydrophobic amino acid residues, the rate limiting step in proteasome proteolysis (Kisselev et al. 1999; Lee and Goldberg 1998). It is possible L7M1 muscle that is LMP7 deficient increased  $\beta 5$  expression to compensate for the loss of LMP7; or more specifically, reduced chymotrypsin-like activity. However,  $\beta 5$  content continued to increase despite no evidence of oxidative damage being present 3 days after the downhill run. This exaggerated response may be due to other factors not measured in the current study, such as L7M1 muscle generating more misfolded or ubiquitinated proteins in the days post-exercise. It is also worth noting that content of the regulatory complexes (i.e., PA28 $\alpha$ , Rpt1) and  $\alpha 7$  did not mirror that of the catalytic subunits. It is possible total proteasome content (i.e.,  $\alpha 7$ ) did not drastically change but rather the 20S core was transformed to cope with the stress associated with the unaccustomed exercise, in which case the regulatory complexes would not be needed (Davies 2001; Jung and Grune 2008). Another possibility is that we missed potential changes in these subunits due to the time points selected. Clearly, the proteasome is a dynamic structure wherein the functional roles of the immunoproteasome and standard proteasome overlap. Further research will be needed to discern how these changes altered the proteasome's catalytic activity and if more intense injury protocols further impact the proteasome's composition.

In closing, we demonstrate the immunoproteasome of skeletal muscle, in particular LMP7, is upregulated in response to unaccustomed exercise, in which the muscle performs eccentric contractions. Furthermore, when LMP7/MECL1 is knocked out, the muscle appears to compensate by increasing  $\beta 5$  content, the catalytic counterpart

of LMP7. These findings indicate the immunoproteasome is sensitive to eccentric contractions and that the inducible subunits influence proteasome content following acute muscular stress. Taken together, these data support previous reports that suggest the immunoproteasome is involved in maintaining cellular homeostasis.

#### ACKNOWLEDGEMENTS

Funding: This study was supported by the Elaine and Robert Larson Endowed Vision Research Chair (to DAF), the National Institutes of Health/ National Institute of Aging (T32-AG29796 to CWB), an anonymous benefactor for Macular Degeneration Research, the Lindsay Family Foundation and an unrestricted grant from Research to Prevent Blindness to the Department of Ophthalmology and Visual Neurosciences. The funders had no role in study design, data collection and analysis, decision to publish or preparation of the manuscript.

## REFERENCES

- Armstrong R, Ogilvie R, Schwane J (1983) Eccentric exercise-induced injury to rat skeletal muscle. *Journal of Applied Physiology* 54:80-93
- Attaix D, Ventadour S, Codran A, Béchet D, Taillandier D, Combaret L (2005) The ubiquitin–proteasome system and skeletal muscle wasting. *Essays in Biochemistry* 41:173-186
- Basler M, Dajee M, Moll C, Groettrup M, Kirk CJ (2010) Prevention of experimental colitis by a selective inhibitor of the immunoproteasome. *The Journal of Immunology* 185:634-641
- Baumann CW, Green MS, Doyle JA, Rupp JC, Ingalls CP, Corona BT (2014a) Muscle injury after low-intensity downhill running reduces running economy. *The Journal of Strength & Conditioning Research* 28:1212-1218
- Baumann CW, Kwak D, Liu HM, Thompson LV (2016a) Age-induced oxidative stress: How does it influence skeletal muscle quantity and quality? *Journal of Applied Physiology* 121:1047-1052
- Baumann CW, Liu HM, Thompson LV (2016b) Denervation-induced activation of the ubiquitin-proteasome system reduces skeletal muscle quantity not quality. *PloS One* 11:e0160839
- Baumann CW, Rogers RG, Gahlot N, Ingalls CP (2014b) Eccentric contractions disrupt FKBP12 content in mouse skeletal muscle. *Physiological Reports* 2:e12081
- Baumann CW, Rogers RG, Otis JS (2016c) Utility of 17-(allylamino)-17-demethoxygeldanamycin treatment for skeletal muscle injury. *Cell Stress and Chaperones* 21:1111-1117
- Baumann CW, Rogers RG, Otis JS, Ingalls CP (2016d) Recovery of strength is dependent on mTORC1 signaling after eccentric muscle injury. *Muscle & Nerve* 54:914-924
- Bedford L, Paine S, Sheppard PW, Mayer RJ, Roelofs J (2010) Assembly, structure, and function of the 26S proteasome. *Trends in Cell Biology* 20:391-401
- Bhattarai S et al. (2016) The immunoproteasomes are key to regulate myokines and MHC class I expression in idiopathic inflammatory myopathies. *Journal of Autoimmunity* 75:118-129
- Brooks SV, Faulkner JA (1988) Contractile properties of skeletal muscles from young, adult and aged mice. *The Journal of Physiology* 404:71-82
- Brooks SV, Zerba E, Faulkner JA (1995) Injury to muscle fibres after single stretches of passive and maximally stimulated muscles in mice. *The Journal of Physiology* 488:459-469
- Chan S, Head S, Morley J (2007) Branched fibers in dystrophic mdx muscle are associated with a loss of force following lengthening contractions. *American Journal of Physiology-Cell Physiology* 293:C985-C992
- Chan S, Seto JT, MacArthur DG, Yang N, North K, Head S (2008) A gene for speed: contractile properties of isolated whole EDL muscle from an  $\alpha$ -actinin-3 knockout mouse. *American Journal of Physiology-Cell Physiology* 295:C897-C904
- Chen C-nJ, Graber TG, Bratten WM, Ferrington DA, Thompson LV (2014) Immunoproteasome in animal models of Duchenne muscular dystrophy. *Journal of Muscle Research & Cell Motility* 35:191-201
- Corona BT, Balog EM, Doyle JA, Rupp JC, Luke RC, Ingalls CP (2010) Junctophilin damage contributes to early strength deficits and EC coupling failure after eccentric contractions. *American Journal of Physiology-Cell Physiology* 298:C365-C376

- Coux O, Tanaka K, Goldberg AL (1996) Structure and functions of the 20S and 26S proteasomes. *Annual Review of Biochemistry* 65:801-847
- Cui Z, Hwang SM, Gomes AV (2014) Identification of the immunoproteasome as a novel regulator of skeletal muscle differentiation. *Molecular and Cellular Biology* 34:96-109
- Dalle-Donne I, Rossi R, Giustarini D, Milzani A, Colombo R (2003) Protein carbonyl groups as biomarkers of oxidative stress. *Clinica Chimica Acta* 329:23-38
- Davies KJ (2001) Degradation of oxidized proteins by the 20S proteasome. *Biochimie* 83:301-310
- Farini A et al. (2016) Therapeutic potential of immunoproteasome inhibition in duchenne muscular dystrophy. *Molecular Therapy* 24:1898-1912
- Ferrington DA, Gregerson DS (2012) Immunoproteasomes: structure, function, and antigen presentation. *Progress in Molecular Biology and Translational Science* 109:75
- Ferrington DA, Husom AD, Thompson LV (2005) Altered proteasome structure, function, and oxidation in aged muscle. *The FASEB Journal* 19:644-646
- Husom AD, Peters EA, Kolling EA, Fugere NA, Thompson LV, Ferrington DA (2004) Altered proteasome function and subunit composition in aged muscle. *Archives of Biochemistry and Biophysics* 421:67-76
- Hussong SA, Kappahn RJ, Phillips SL, Maldonado M, Ferrington DA (2010) Immunoproteasome deficiency alters retinal proteasome's response to stress. *Journal of Neurochemistry* 113:1481-1490
- Hussong SA, Roehrich H, Kappahn RJ, Maldonado M, Pardue MT, Ferrington DA (2011) A novel role for the immunoproteasome in retinal function. *Investigative Ophthalmology & Visual Science* 52:714-723
- Ichikawa HT et al. (2012) Beneficial effect of novel proteasome inhibitors in murine lupus via dual inhibition of type I interferon and autoantibody-secreting cells. *Arthritis & Rheumatology* 64:493-503
- Ingalls CP, Warren GL, Armstrong R (1998a) Dissociation of force production from MHC and actin contents in muscles injured by eccentric contractions. *Journal of Muscle Research & Cell Motility* 19:215-224
- Ingalls CP, Warren GL, Williams JH, Ward CW, Armstrong R (1998b) EC coupling failure in mouse EDL muscle after in vivo eccentric contractions. *Journal of Applied Physiology* 85:58-67
- Ingalls CP, Wenke J, Nofal T, Armstrong R (2004) Adaptation to lengthening contraction-induced injury in mouse muscle. *Journal of Applied Physiology* 97:1067-1076
- Jones D, Howell S, Roussos C, Edwards R (1982) Low-frequency fatigue in isolated skeletal muscles and the effects of methylxanthines. *Clinical Science (London, England: 1979)* 63:161-167
- Jung T, Grune T (2008) The proteasome and its role in the degradation of oxidized proteins. *IUBMB Life* 60:743-752
- Kisselev AF, Akopian TN, Castillo V, Goldberg AL (1999) Proteasome active sites allosterically regulate each other, suggesting a cyclical bite-chew mechanism for protein breakdown. *Molecular Cell* 4:395-402
- Kloetzel P-M (2001) Antigen processing by the proteasome. *Nature Reviews Molecular Cell Biology* 2:179-188
- Lecker SH, Goldberg AL, Mitch WE (2006) Protein degradation by the ubiquitin-proteasome pathway in normal and disease states. *Journal of the American Society of Nephrology* 17:1807-1819

- Lecker SH, Solomon V, Mitch WE, Goldberg AL (1999) Muscle protein breakdown and the critical role of the ubiquitin-proteasome pathway in normal and disease states. *The Journal of Nutrition* 129:227S-237S
- Lee DH, Goldberg AL (1998) Proteasome inhibitors: valuable new tools for cell biologists. *Trends in Cell Biology* 8:397-403
- Liu HM, Ferrington DA, Baumann CW, Thompson LV (2016) Denervation-induced activation of the standard proteasome and immunoproteasome. *PloS One* 11:e0166831
- López JR, Mijares A, Kolster J, Henriquez-Olguin C, Zhang R, Altamirano F, Adams JA (2016) Whole body periodic acceleration improves muscle recovery after eccentric exercise. *Medicine and Science in Sports and Exercise* 48:1485-1494
- Lowe DA, Warren GL, Ingalls CP, Boorstein DB, Armstrong R (1995) Muscle function and protein metabolism after initiation of eccentric contraction-induced injury. *Journal of Applied Physiology* 79:1260-1270
- Lueders TN et al. (2011) The  $\alpha 7\beta 1$ -integrin accelerates fiber hypertrophy and myogenesis following a single bout of eccentric exercise. *American Journal of Physiology-Cell Physiology* 301:C938-C946
- Lynch GS, Fary CJ, Williams DA (1997) Quantitative measurement of resting skeletal muscle  $[Ca^{2+}]_i$  following acute and long-term downhill running exercise in mice. *Cell Calcium* 22:373-383
- McArdle A, Dillmann WH, Mestral R, Faulkner JA, Jackson MJ (2004) Overexpression of HSP70 in mouse skeletal muscle protects against muscle damage and age-related muscle dysfunction. *The FASEB Journal* 18:355-357
- Méndez J, Keys A (1960) Density and composition of mammalian muscle. *Metabolism-Clinical and Experimental* 9:184-188
- Muchamuel T et al. (2009) A selective inhibitor of the immunoproteasome subunit LMP7 blocks cytokine production and attenuates progression of experimental arthritis. *Nature Medicine* 15:781-787
- Pizza FX, Koh TJ, McGregor SJ, Brooks SV (2002) Muscle inflammatory cells after passive stretches, isometric contractions, and lengthening contractions. *Journal of Applied Physiology* 92:1873-1878
- Rathbone CR, Wenke J, Warren GL, Armstrong R (2003) Importance of satellite cells in the strength recovery after eccentric contraction-induced muscle injury. *American Journal of Physiology-Regulatory, Integrative and Comparative Physiology* 285:R1490-R1495
- Reid MB (2005) Response of the ubiquitin-proteasome pathway to changes in muscle activity. *American Journal of Physiology-Regulatory, Integrative and Comparative Physiology* 288:R1423-R1431
- Schuld NJ et al. (2015) Immunoproteasome deficiency protects in the retina after optic nerve crush. *PloS One* 10:e0126768
- Schwane JA, Johnson SR, Vandenaeker CB, Armstrong RB (1982) Delayed-onset muscular soreness and plasma CPK and LDH activities after downhill running. *Medicine and Science in Sports and Exercise* 15:51-56
- Seifert U et al. (2010) Immunoproteasomes preserve protein homeostasis upon interferon-induced oxidative stress. *Cell* 142:613-624
- Tanaka K (2009) The proteasome: Overview of structure and functions. *Proceedings of the Japan Academy, Series B* 85:12-36

- Tanaka K, Kasahara M (1998) The MHC class I ligand generating system: Roles of immunoproteasomes and the interferon-gamma-inducible proteasome activator PA28. *Immunological Reviews* 163:161-176
- Wang H et al. (2016) Increasing regulatory T cells with interleukin-2 and interleukin-2 antibody complexes attenuates lung inflammation and heart failure progression. *Hypertension* 68:114-122
- Warren GL, Hayes D, Lowe D, Armstrong R (1993a) Mechanical factors in the initiation of eccentric contraction-induced injury in rat soleus muscle. *The Journal of Physiology* 464:457
- Warren GL, Lowe DA, Hayes DA, Karwoski CJ, Prior BM, Armstrong R (1993b) Excitation failure in eccentric contraction-induced injury of mouse soleus muscle. *The Journal of Physiology* 468:487-499
- Westerblad H, Duty S, Allen D (1993) Intracellular calcium concentration during low-frequency fatigue in isolated single fibers of mouse skeletal muscle. *Journal of Applied Physiology* 75:382-388
- Willoughby DS, Taylor M, Taylor L (2003) Glucocorticoid receptor and ubiquitin expression after repeated eccentric exercise. *Medicine and Science in Sports and Exercise* 35:2023-2031

## FIGURE LEGENDS

**Fig. 1. Descriptive characteristics of the controls.** Baseline (A) body weight, (B) body fat %, (C) muscle weight, (D) fiber CSA, and peak isometric (E) twitch and (F) tetanic force were assessed in control (non-exercised) mice. All mice were male and 8-16 weeks of age, with exception to body fat % (see Methods). Body fat % was determined using a Lunar PIXImus densitometer. Fiber cross-sectional area (CSA) was done by averaging the CSA of approximately 200 fibers from the soleus muscle of each mouse. Soleus peak isometric twitch ( $P_t$ ) and tetanic ( $P_o$ ) force were assessed *ex vivo* and set relative to physiological CSA. Sample size per group,  $n=9-10$  for body fat %. For all other variables,  $n=5-7$ . Values are mean $\pm$ SEM. \*Strains are significantly different ( $p<0.05$ ).

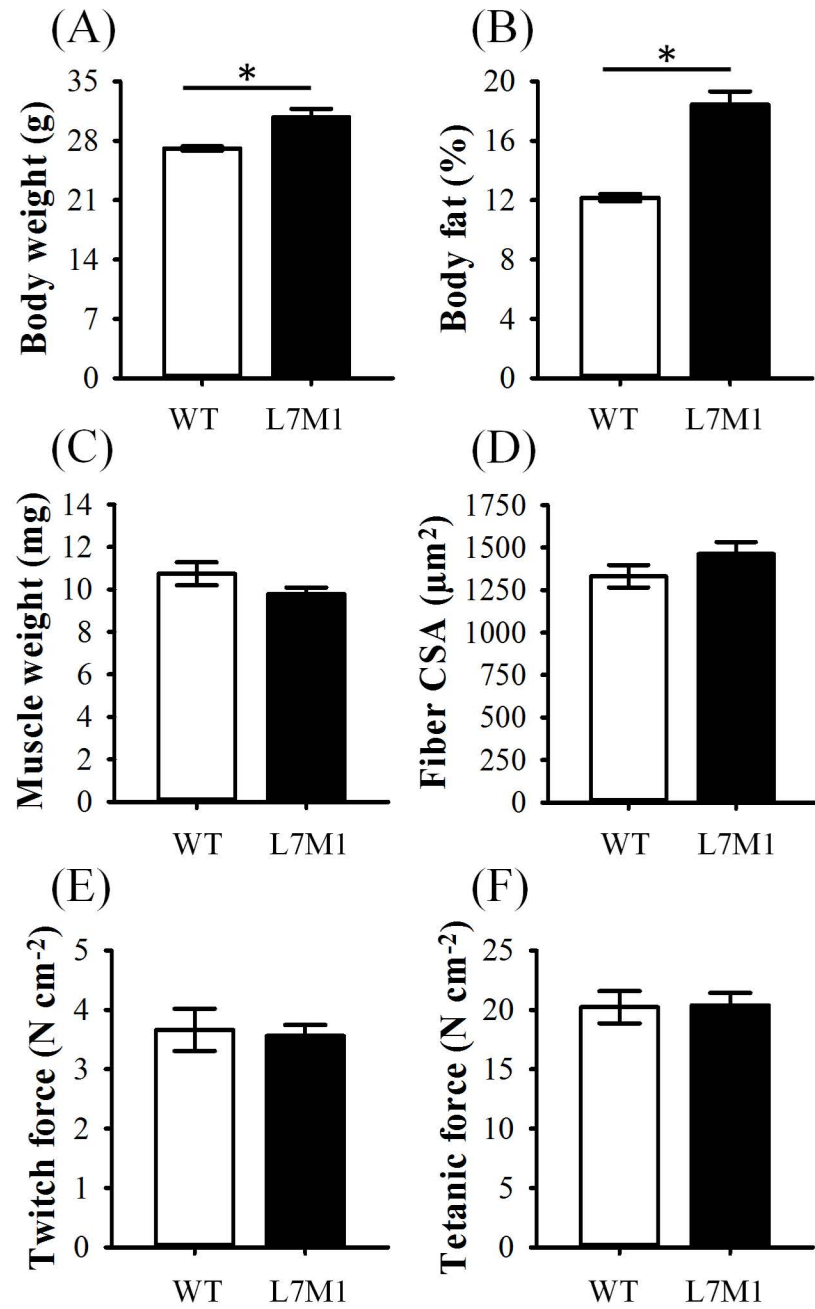
**Fig. 2. *Ex vivo* contractile function.** Peak isometric (A) twitch and (B) tetanic force were determined from the soleus muscle and are referred to as  $P_t$  and  $P_o$  within the text. The ratio of (C) twitch to tetanic force was calculated by dividing  $P_t$  by  $P_o$ . The (D)  $Freq_{50}$  was determined from the (E) force-frequency relationship, which was fit with a Hill sigmoidal curve. All values are expressed as a % difference from each groups' respective control. The control groups consisted of soleus muscle from mice that did not exercise. Day 1 and Day 3 groups included soleus muscle from mice that ran for 70 min on a motorized treadmill set at a negative grade (downhill). These mice were then tested either 1 day (Day 1) or 3 days (Day 3) post-exercise. Sample size per group,  $n=5-7$ . Values are mean $\pm$ SEM. Bars with different letter(s) represent a significant main effect of time ( $p<0.05$ ).  $P_t$ , peak isometric twitch force;  $P_o$ , peak isometric tetanic force;  $Freq_{50}$ , frequency at which 50% of  $P_o$  was reached.

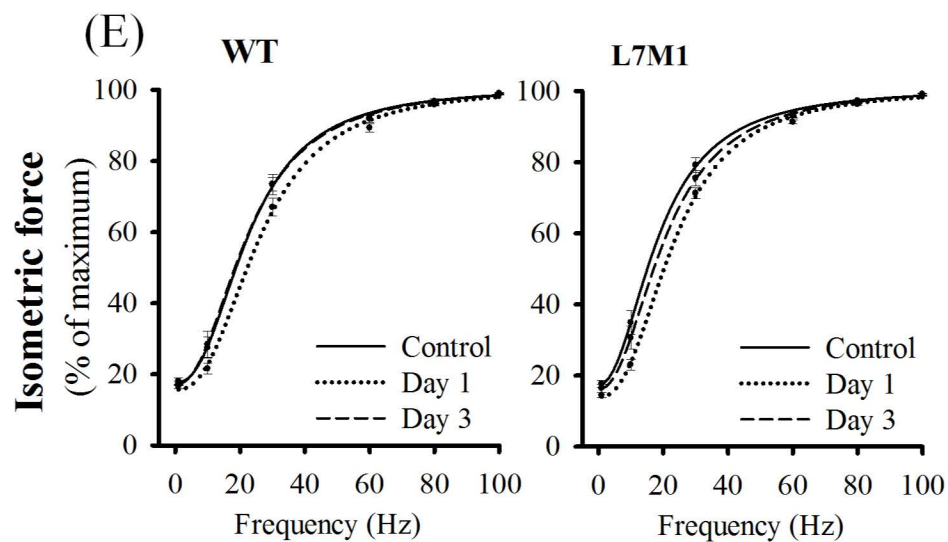
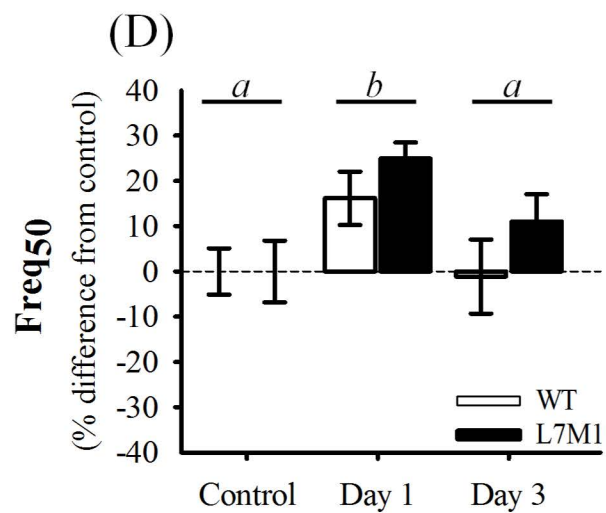
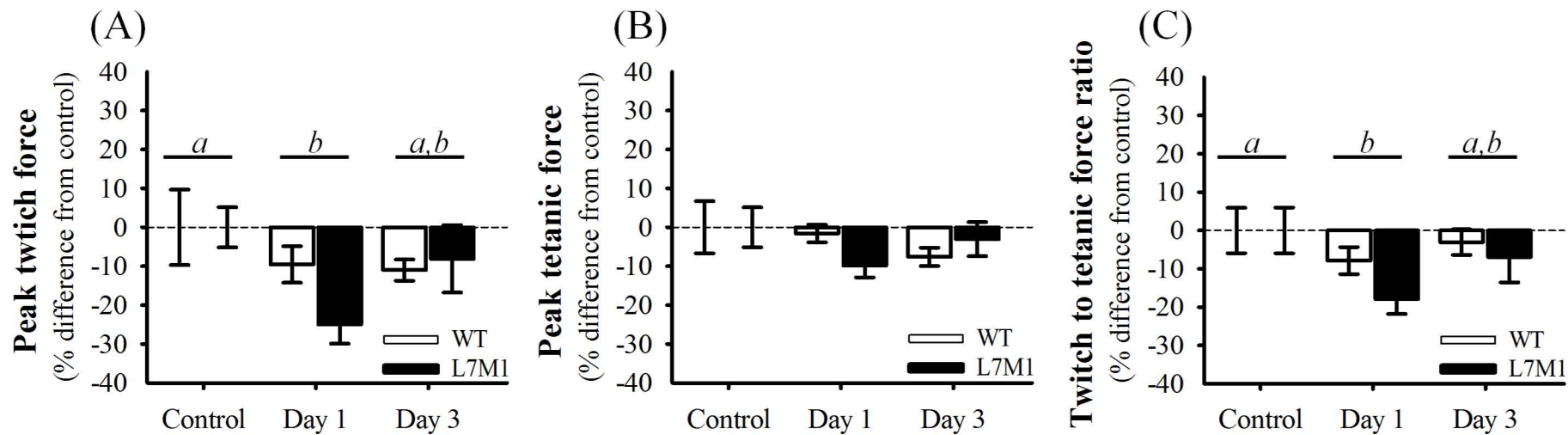
**Fig. 3. Proteasome content.** Content of the (A, B, E) immunoproteasome, (C, D, F) standard proteasome and (G) total proteasome of the soleus muscle were determined using Western blot analysis. A representative blot of each protein of interest is depicted in panel H. Proteins were normalized to GAPDH and expressed as a fraction of each groups' respective control. The control groups consisted of soleus muscle from mice that did not exercise. Day 1 and Day 3 groups included soleus muscle from mice that ran for 70 min on a motorized treadmill set at a negative grade (downhill). These mice were then tested either 1 day (Day 1) or 3 days (Day 3) post-exercise. Sample size per group,  $n=5-7$ . Values are mean $\pm$ SEM. Circles with different letter(s) represent a significant main effect of time ( $p<0.05$ ). \*Significant main effect of strain ( $p<0.05$ ).

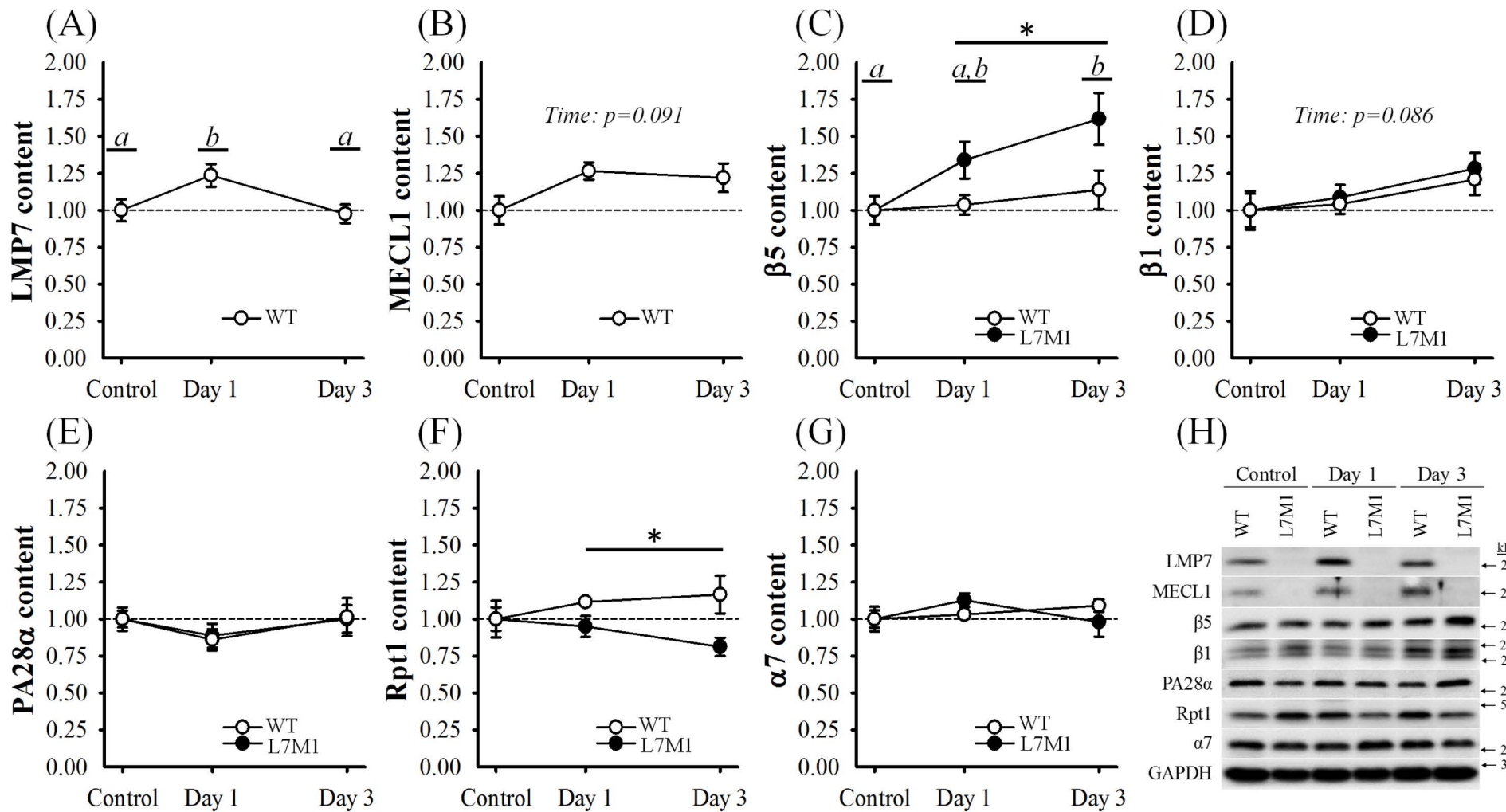
**Fig. 4. Inflammatory response.** Content of (A) MCP1 and (B)  $TNF\alpha$ , and the (C) percentage of CD45 positively stained cells were used to determine if the bout of downhill running triggered an inflammatory response in the soleus muscle of WT and L7M1 mice. Content of (A) MCP1 and (B)  $TNF\alpha$  were determined using ELISA kits, while the percentage of CD45 positively stained cells was analyzed using immunohistochemistry. A representative picture of the immunostains from each group is depicted in **Supplementary Fig. 1A**. All values are expressed as a fraction of each groups' respective control. The control groups consisted of soleus muscle from mice that did not exercise. Day 1 and Day 3 groups included soleus muscle from mice that ran for 70 min on a motorized treadmill set at a negative grade (downhill). These mice were then tested either 1 day (Day 1) or 3 days (Day 3) post-exercise. Sample size per group,  $n=5-7$ . Values are mean $\pm$ SEM.

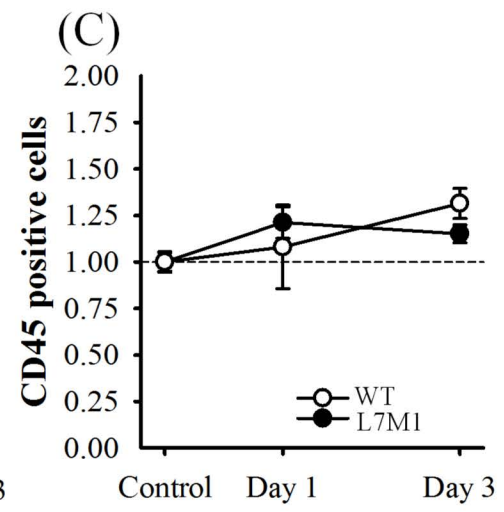
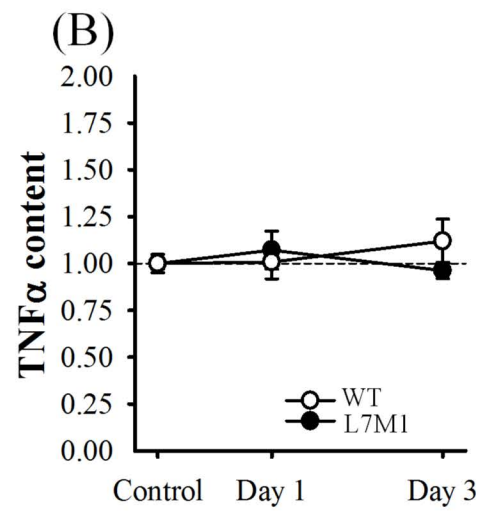
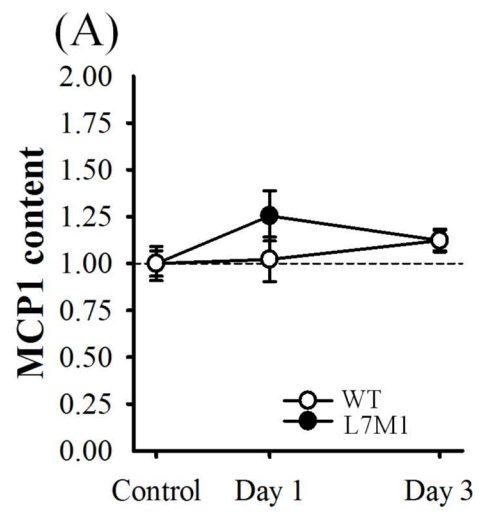
**Fig. 5. Protein carbonylation.** Oxidative stress was estimated by determining protein carbonylation content in (A) total (i.e., whole membrane) and for three prominent bands (Figure 4A to 4D) from the soleus muscle via Western blot analysis. These bands were approximately at (B) 220, (C) 40 and (D) 30 kDa. A representative blot is depicted in panel E. Protein carbonylation was normalized to GAPDH and expressed as a fraction of each groups' respective control. The control groups consisted of soleus muscle from mice that did not exercise. Day 1 and Day 3 groups included soleus muscle from mice that ran for 70 min on a motorized treadmill set at a negative grade (downhill). These mice were then tested either 1 day (Day 1) or 3 days (Day 3) post-exercise. Sample size per group,  $n=5-7$ . Values are mean $\pm$ SEM. Circles with different letter(s) represent a significant main effect of time ( $p<0.05$ ). DNP, 2,4-dinitrophenyl.

**Supplementary Fig. 1. Representative CD45 immunostains.** Quantitative values are depicted in **Fig. 4C**.

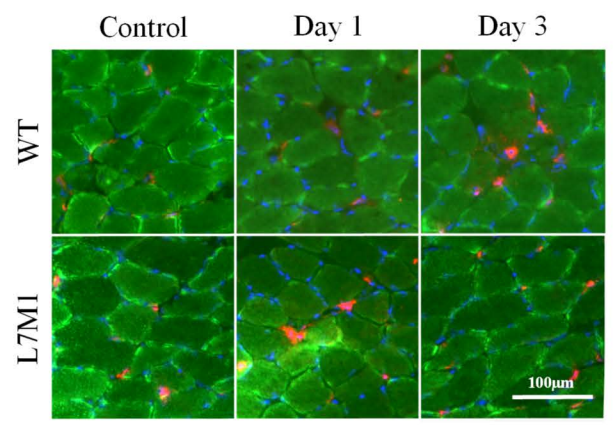












Supplementary Table 1. Primary antibodies used for Western blotting

Primary antibody	Dilution	Manufacturer	Product number
Proteasome 20S $\beta$ 5i (LMP7)	1:2000	Enzo Life Sciences, Farmingdale, NY	#PW8200
Proteasome 20S $\beta$ 2i (MECL1)	1:1000	Enzo Life Sciences, Farmingdale, NY	#PW8150
Proteasome 20S $\beta$ 5, PSMB5	1:1000	Thermo Scientific, Rockford, IL	#PA1-977
Proteasome 20S $\beta$ 1, PSMB6	1:1000	Thermo Scientific, Rockford, IL	#PA1-978
Proteasome 11S (PA28 $\alpha$ )	1:1000	Enzo Life Sciences, Farmingdale, NY	#PW8185
Proteasome 19S Rpt1/S7	1:1000	Enzo Life Sciences, Farmingdale, NY	#PW9400
Proteasome 20S $\alpha$ 7	1:1000	Enzo Life Sciences, Farmingdale, NY	#PW8110
GAPDH	1:4000	Cell Signaling Technology, Danvers, MA	#3683

Supplementary Table 2. Contractile and inflammatory characteristics of the soleus muscle.

	WT			L7M1		
	Control	Day 1	Day 3	Control	Day 1	Day 3
P <sub>t</sub> (N·cm <sup>-2</sup> )	3.66±0.36	3.31±0.17	3.26±0.10	3.56±0.18	2.67±0.18	3.27±0.31
P <sub>o</sub> (N·cm <sup>-2</sup> )	20.23±1.35	19.91±0.46	18.69±0.47	20.38±1.05	18.38±0.62	19.76±0.90
P <sub>t</sub> /P <sub>o</sub> (ratio)	0.180±0.01	0.166±0.01	0.175±0.01	0.177±0.01	0.145±0.01	0.165±0.01
MCP1 (pg/ml)	19.47±1.31	19.90±2.32	21.86±1.19	18.52±1.69	23.22±2.49	20.79±1.01
TNFα (pg/ml)	105.87±3.10	106.72±9.59	118.54±12.42	110.01±5.36	117.91±11.18	105.86±4.80
CD45 (%)	4.90±0.24	5.29±1.10	6.44±0.40	5.74±0.32	6.95±0.49	6.61±0.28

Values are means±SEM. Sample size per group, n=5-7. The control groups consisted of soleus muscle that were not exercised. Day 1 and Day 3 groups included soleus muscle from mice that had run for 70 min on a motorized treadmill set at a negative grade (downhill). These mice were then tested either 1 day (Day 1) or 3 days (Day 3) post-exercise. L7M1 are double knockout *Imp7*<sup>-/-</sup> and *mecl1*<sup>-/-</sup> mice with a C57BL/6 (wildtype; WT) genetic background. P<sub>t</sub>, peak isometric twitch force; P<sub>o</sub>, peak isometric tetanic force.